J Biomol NMR (2007) 37:195–204
DOI 10.1007/s10858-006-9120-z

ARTICLE

Mixed-time parallel evolution in multiple quantum NMR experiments: sensitivity and resolution enhancement in heteronuclear NMR

Jinfa Ying · Jordan H. Chill · John M. Louis · Ad Bax

Received: 13 October 2006 / Accepted: 21 November 2006 / Published online: 24 January 2007
© Springer Science+Business Media B.V. 2007

Abstract A new strategy is demonstrated that simultaneously enhances sensitivity and resolution in three- or higher-dimensional heteronuclear multiple quantum NMR experiments. The approach, referred to as mixed-time parallel evolution (MT-PARE), utilizes evolution of chemical shifts of the spins participating in the multiple quantum coherence in parallel, thereby reducing signal losses relative to sequential evolution. The signal in a given PARE dimension, t_1, is of a non-decaying constant-time nature for a duration that depends on the length of t_2, and vice versa, prior to the onset of conventional exponential decay. Line shape simulations for the ^{1}H–^{15}N PARE indicate that this strategy significantly enhances both sensitivity and resolution in the indirect ^{1}H dimension, and that the unusual signal decay profile results in acceptable line shapes. Incorporation of the MT-PARE approach into a 3D HMQC-NOESY experiment for measurement of H^N–H^N NOEs in KcsA in SDS micelles at 50°C was found to increase the experimental sensitivity by a factor of 1.7±0.3 with a concomitant resolution increase in the indirectly detected ^{1}H dimension. The method is also demonstrated for a situation in which homonuclear ^{13}C–^{13}C decoupling is required while measuring weak H3′–2′OH NOEs in an RNA oligomer.

Keywords KcsA · Mixed-time · Multiple quantum NMR · NOESY · Parallel evolution · Resolution enhancement · RNA · Sensitivity enhancement

Introduction

Over the past decades, efforts to enhance sensitivity of NMR experiments have played an essential role in the development of methodology suitable for the study of larger proteins and biomolecular complexes. Of the various approaches taken, the favorable relaxation properties of one-bond ^{1}H–^{15}N and ^{1}H–^{13}C multiple quantum coherence have proven to be particularly useful to simultaneously enhance both sensitivity and spectral resolution (Griffey and Redfield 1987; Bax et al. 1989; Grzesiek and Bax 1995; Marino et al. 1997; Shang et al. 1997; Gschwind et al. 1998). During certain 3D constant-time experiments, evolution of such multiple quantum coherences permits the use of a single delay to simultaneously record chemical shift evolution of both nuclei participating in the multiple quantum coherence (Pervushin and Eletsky 2003; Ying and Bax 2006), thereby further reducing signal losses relative to the use of sequential evolution periods. We refer to this approach as parallel evolution (PARE), emphasizing that the chemical shifts of the nuclei involved in the multiple quantum coherence evolve independently and *in parallel* in the indirect dimensions of the experiment. In constant-time NMR experiments, the PARE strategy to record chemical shifts in multiple indirect dimensions can be implemented straightforwardly (Pervushin and Eletsky 2003; Ying and Bax 2006). Here we demonstrate that the PARE approach is also applicable in regular,

Electronic Supplementary Material The online version of this article (doi:10.1007/s10858-006-9120-z) contains supplementary material, which is available to authorized users.

J. Ying · J. H. Chill · J. M. Louis · A. Bax
Laboratory of Chemical Physics, National Institute of Diabetes and Digestive and Kidney Diseases, National Institutes of Health, Bethesda, MD 20892, USA

non-constant-time NMR experiments, offering simultaneous enhancements in resolution and sensitivity.

The new 3D PARE experiments can be considered as hybrids of the conventional, sequential evolution period methods and the above mentioned constant-time PARE experiments. In the new experiment, as soon as the evolution period of the multi-quantum duration is incremented to become non-zero, this period is utilized simultaneously for evolution of both nuclei. The 3D time domain signal, obtained in this manner, has an unusual decay profile in that it is of a non-decaying, constant-time nature in the t_2 dimension for a duration that depends on t_1; vice versa, t_1 decay is absent for a constant-time duration that depends on t_2, prior to commencing regular exponential decay. We refer to this way of recording chemical shifts as a mixed-time (MT) approach, and it is analogous to the widely used semi-constant-time method (Grzesiek et al. 1993; Logan et al. 1993), but results in a discontinuity in the time domain decay profile. Although this discontinuity results in a non-Lorentzian line shape, this line shape actually shows resolution-enhanced behavior with minimal baseline distortion. The MT-PARE evolution concept is demonstrated for recording 3D ^{15}N-separated NOESY spectra on the transmembrane domain of the tetrameric KcsA potassium channel in SDS detergent micelles, and for recording ^{13}C-separated NOESY data to hydroxyl protons in a 24-nt stem-loop RNA structure.

Materials and methods

Sample preparation

Expression, purification, and NMR sample preparation of tetrameric, uniformly ^{2}H/^{13}C/^{15}N-enriched bacterial potassium channel from *Streptomyces lividens* (KcsA) spanning residues 16–160 has been described previously (Chill et al. 2006b). KcsA was expressed in H_2O-based minimal medium supplemented with deuterated nutrients and transferred during purification to D_2O. This afforded a KcsA sample in which only the non-exchangeable backbone amides with very rapid transverse relaxation rates, mainly located in the transmembrane helices are observable (Chill et al. 2006b). The sample contained 0.2 mM KcsA (tetramer concentration), 150 mM SDS, 20 mM Tris buffer in 99% D_2O, pH 8.0 (uncorrected), and has a total volume of 275 µl in a Shigemi thin-wall microcell.

The RNA sample contained 1.0 mM solution of the uniformly ^{13}C/^{15}N-enriched oligomer GGGCUA-AUGψUGAAAAAUUAGCCC, corresponding to nucleotides 737–760 of helix-35 in *E. coli* 23S ribosomal RNA. In this oligonucleotide, ψ746 refers to pseudouridine. The sample was prepared as described elsewhere (Nikonowicz et al. 1992), and contained 10 mM phosphate buffer, pH 6.8, 10 mM NaCl, 0.02 mM EDTA, in 300 µl 95% H_2O/5%D_2O, in a Shigemi thin-wall microcell.

Data acquisition and processing

All NMR spectra were acquired on a Bruker DRX800 spectrometer, equipped with a cryogenic triple-resonance probehead containing a *z*-axis pulsed field gradient accessory. For all comparisons, the experiment employing the MT-PARE evolution strategy was always executed sequentially with the corresponding reference, conventional MQ experiment, using otherwise identical acquisition parameters. For the H^N–H^N NOESY spectrum of the hydrogen-exchange-protected backbone amide protons of the KcsA transmembrane domain (KcsA^{TM}), recorded in D_2O at 50°C, an NOE mixing time of 80 ms was used. Each KcsA spectrum was acquired as a $89^* \times 39^* \times 512^*$ data matrix, with acquisition times of 27.5 ms (t_1, ^{1}H), 19.5 ms (t_2, ^{15}N), and 40.0 ms (t_3, ^{1}H), using 8 transients per FID and a 1.5 s delay between scans, resulting in total measurement times of ca 57 h each. The spectral width in the F_2 (^{15}N) dimension was 24 ppm, with the carrier centered at 117.1 ppm, and in the F_1 (^{1}H) dimension peaks were folded into a region of 4.0 ppm, centered on the residual HOD peak. Spectra were processed and analyzed using the NMRPipe software package (Delaglio et al. 1995). A 90°-shifted sine-squared function, truncated at 176.4°, was used to apodize the directly detected time domain data, whereas for the two indirect time domain data a 90°-shifted sine bell function truncated at 176.4° was applied for each spectrum. Prior to 3D Fourier transformation, the data were zero filled to yield final matrices of $512^*(F_1) \times 256^*(F_2) \times 2048^*(F_3)$ data points. Note that no special routines are needed for processing or converting PARE data and processing scripts are identical to those regularly used for processing 3D data.

The ^{13}C-separated 3D H3′–2′OH NOESY spectra on the RNA sample were recorded with the conventional and MT-PARE approaches. Experiments were carried out in H_2O at 7°C to minimize solvent exchange of the hydroxyl protons. A NOE mixing time of 40 ms was used. Each spectrum was acquired as a $50^* \times 65^* \times 512^*$ data matrix with acquisition times of 28.9 ms (t_1, ^{1}H), 22 ms (t_2, ^{13}C), and 64 ms (t_3, ^{1}H), using 8 transients per FID and a 1.65 s delay per transient, for a total measurement time of 55 h per 3D

spectrum. The spectral width in the $F_2(^{13}C)$ dimension was 14.5 ppm, centered at 72.7 ppm, and in the $F_1(^1H)$ dimension the spectral width was 2.1 ppm, centered on the water peak. The spectra were processed and analyzed in the same way as described above for KcsA. The final matrix in each 3D spectrum contained $256^*(F_1) \times 512^*(F_2) \times 2048^*(F_3)$ data points.

Line shape simulation

In the MT type of experiments, magnetization does not decay exponentially, which may distort the resulting line shape after Fourier transform. To investigate the effect of the MT chemical shift evolution on the line shape, we simulated the line shapes in the two indirect dimensions obtained both in our PARE and conventional MQ H^N–H^N NOESY experiments. In the simulation, the T_2 for the single quantum ^1H magnetization was set to 10 ms, whereas a slightly longer T_2 (12 ms) was used for the ^1H–^{15}N multiple quantum coherence. These transverse relaxation times were based on approximate measurements made for the amide groups in the transmembrane domain of the tetrameric KcsA in SDS micelle solution at 50°C in D_2O, for which a rotational correlation time of ca 50 ns has been reported (Chill et al. 2006a). Without loss of generality, we assume both ^1H and ^{15}N signals to be on resonance. The real part of the FIDs in each one of the two dimensions was then calculated from the T_2 values as well as the total time durations at each point of the indirect acquisition, whereas the imaginary part for the on-resonance signals equals zero. A matrix of the simulated complex data was then generated in the format of a Bruker serial file, and finally processed with the NMRPipe software package (Delaglio et al. 1995). The spectral widths and number of points in the indirect dimensions of the data set were the same as described above for the KcsA NOESY experiment. For comparison, an analogous time domain signal was generated for the conventional HMQC-NOESY spectrum, mimicking the experimental reference spectrum.

Results and discussion

Concept and implementation of mixed-time parallel evolution (MT-PARE)

The parallel evolutions of two spins during a multiple quantum period have the largest relaxation advantage in cases where one of the two spins is a proton. Measurement of the ^1H frequency during such MQ evolution is most advantageous in ''uni-directional'' experiments, such as NOESY, or uni-directional *J*-correlation experiments. For the so-called ''out-and-back'' experiments (Ikura et al. 1990), the ^1H frequency is already available during the detected dimension, and therefore its separate measurement in the indirect dimension in most cases would be redundant. Therefore, we choose to illustrate the implementation and utility of the MT-PARE approach for the all-important NOESY experiment, where both sensitivity and resolution are frequently the limiting factors during analysis, and the enhancements offered by MT-PARE are most important. In the examples discussed below, we focus on H^N–H^N and H3′–2′OH HMQC-NOESY experiments for a protein and RNA, respectively.

The 3D MT-PARE HMQC-NOESY pulse sequences, applied to the protein and RNA, are shown in Figs. 1 and 2. As discussed below, the parallel evolution strategy involves the recording of the evolution in the indirect dimensions in a mixed-time manner, i.e. a combination of constant-time for the initial data points, until the maximum constant-time duration has been fully exploited, and then followed by ''real-time'' incrementation for the remaining data points.

We first discuss in some detail the concept of MT-PARE evolution for the HMQC element that preceded the NOE mixing period in Fig. 1. At time point *a*, transverse magnetization originating from amide protons is converted into ^1H–^{15}N multiple quantum coherence. With the absence of a $^1J_{NH}$ contribution to the zero and double quantum frequencies, present between time points *a* and *b*, ^1H and ^{15}N chemical shift evolution is effected by stepwise movement of the ^1H and ^{15}N 180° pulses, respectively, applied during this period, in full analogy to the parallel evolution experiment of Pervushin and Eletsky (2003). The difference relative to these earlier constant-time experiments is that the MQ duration is only incremented once all available CT evolution has been utilized, i.e., when the composite ^1H 180° pulse during the PARE period and the composite $^1H/^{15}N$ 180° pulse pair during the first δ delay both have reached time point *a* (Fig. 1C). Note that even when $t_2 = 0$, constant-time ^1H evolution is available and utilized for the initial 2δ duration in the t_1 dimension. So, initially for $t_1 = t_2 = 0$, the duration between time points *a* and *b* is set to the minimum value needed to accommodate the 180° ^1H and ^{15}N pulses, refocusing ^1H and ^{15}N chemical shift evolution between time points *a* and *b*, as well as the ^1H chemical shift evolution during the delay 2δ since the pair of 180° $^1H/^{15}N$ composite pulses during the first δ delay initially is applied at the beginning of δ, immediately following the first 90° ^1H pulse. It follows that for $t_2 = 0$, only a duration of 2δ CT evolution is available for

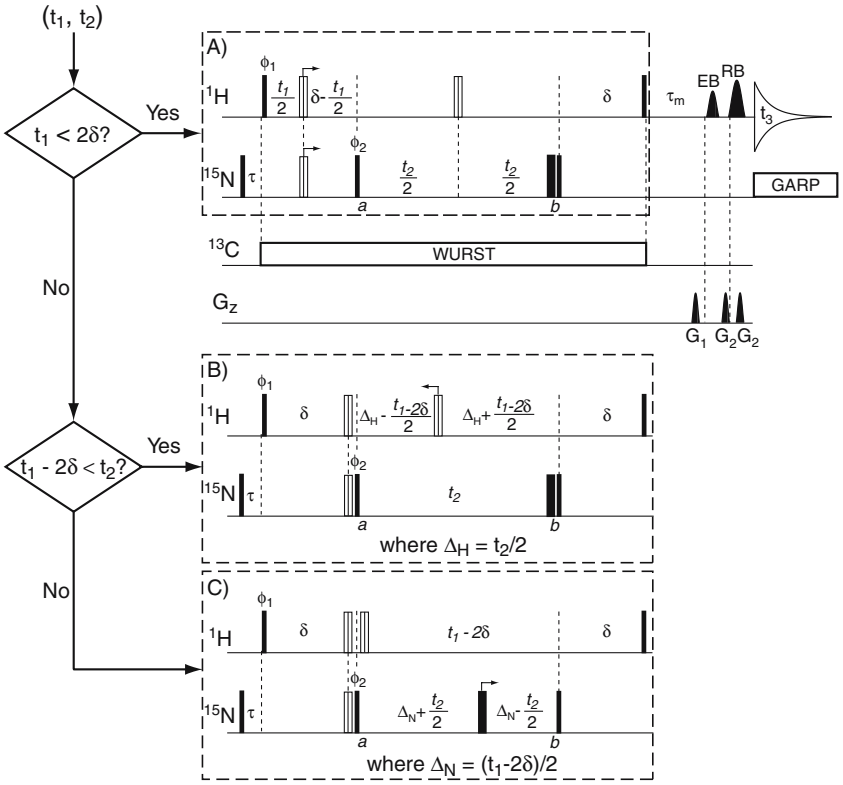

Fig. 1 3D MT-PARE-HMQC-NOESY pulse sequences for measurement of H^N–H^N NOEs in proteins. Narrow and wide filled bars correspond to 90° and 180° pulses, respectively. Vertically hatched open bars represent composite pulses ($90°_x 200°_y 90°_x$ for ^{1}H and $90°_x 220°_y 90°_x$ for ^{15}N) employed to reduce RF inhomogeneity and off-resonance effects. Unless otherwise indicated, all pulses have phase x. Incrementation of the t_1 and t_2 evolution periods is carried out in a manner that depends on the duration of t_1 and t_2, and requires the dashed box scheme of (**A**) for $t_1 < \delta$; (**B**) when $0 < t_1 - 2\delta < t_2$; and (**C**) when $t_1 - 2\delta > t_2$. In (**A**), the shaped pulse labeled EB represents a 90° $^1H^N$ pulse with the EBURP-2 profile (Geen and Freeman 1991), with a duration of 1.2 ms (at 800 MHz ^{1}H frequency), and the pulse labeled RB is a 1.2-ms 180° $^1H^N$ pulse with the REBURP profile. These pulses are centered at 8.28 ppm. Broadband ^{13}C decoupling was achieved using a sequence of adiabatic WURST pulses (Kupče and Freeman 1995) with a sweep width of 28 kHz and ^{13}C WURST pulse durations of 10 ms (at 201 MHz ^{13}C frequency), centered at 117.5 ppm. Phase cycling: $\phi_1 = -x$; $\phi_2 = x, -x$; receiver = x, $-x$. Regular States-TPPI phase cycling of ϕ_1 and ϕ_2 was used to obtain quadrature detection in the ^{1}H (F_1) and ^{15}N (F_2) indirect dimensions, respectively. Delay durations: τ = 50 ms; δ = 4.1 ms; τ_m = 80 ms; $\Delta_N = (t_1 - 2\delta)/2$, i.e. iteratively calculated at each t_1 point during the acquisition, and $\Delta_H = t_2/2$. Pulsed field gradients are sine-bell shaped. The gradient pulses have durations of 2 ms and 1 ms, with peak amplitudes of 20 G/cm and 27 G/cm for G_1 and G_2, respectively. Bruker pulse sequence codes, acquisition parameters, and NMRPipe processing scripts, that are the same as for regular 3D HMQC-NOESY spectra, can be downloaded from < http://spin.niddk.nih.gov/bax >

$^1H^N$; for the remaining data points in the ^{1}H dimension at $t_2 = 0$, incrementation of the duration between a and b by t_1–2δ is required (Fig. 1C). For non-zero t_2 durations, signal decay in the $^1H^N$ dimension starts after $t_1 > 2\delta + t_2$ (see also the cross sections through the simulated time domain signal of Fig. 3D). Note that transverse relaxation of $^1H^N$ during this MQ evolution is slower than during single quantum H^N evolution as it is not affected by the $J(0)$ spectral density terms containing the one-bond ^{1}H–^{15}N dipolar interaction (Griffey and Redfield 1987; Bax et al. 1989).

Conversely, the manner in which the ^{15}N evolution period, t_2, is incremented depends on the duration of t_1. For $t_1 \leq 2\delta$ (Fig. 1A) or $t_1 < t_2 + 2\delta$ (Fig. 1B), real incrementation of t_2 is required, resulting in regular exponential relaxation decay in the ^{15}N dimension. This t_2 decay is present for the region of the time domain where $t_2 > t_1 - 2\delta$ (Fig. 3). However, for $t_2 \leq t_1 - 2\delta$, the chemical shifts in t_2 are recorded in a constant-time fashion (Fig. 1C), permitting the initial t_2 evolution in a constant-time mode, without relaxation decay (Fig. 3C).

Simultaneous elimination during PARE acquisition of both $^1J_{NC}$ and multi-bond $^nJ_{HC}$ couplings in ^{13}C-labeled proteins by application of ^{13}C 180° pulses is rather cumbersome in these experiments. We therefore opted for the far more convenient synchronous

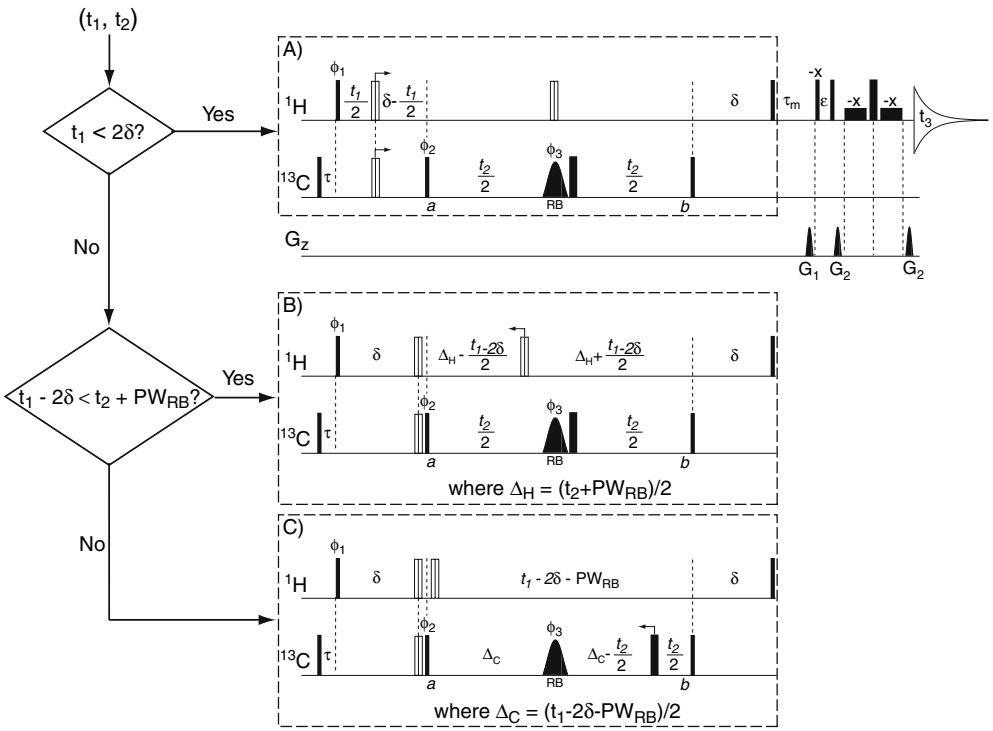

Fig. 2 3D MT-PARE-HMQC-NOESY pulse sequences for measurement H3′–2′OH NOEs in RNA. Narrow and wide filled bars correspond to 90° and 180° pulses, respectively. Vertically hatched open bars represent composite pulses ($90°_x 200°_y 90°_x$ for ^{1}H and $90°_x 220°_y 90°_x$ for ^{13}C). As for the pulse scheme of Fig. 1, which delay is being incremented in the pulse scheme depends on the durations of both t_1 and t_2, switching between the HMQC elements of (**A**), (**B**) and (**C**). The 3-ms 180° ^{13}C shaped pulse (at 201 MHz ^{13}C frequency) labeled "RB" has a REBURP profile (Geen and Freeman 1991) and is centered at 70 ppm in the C3′ region. The $90_{-x} - \varepsilon - 90_x$ module (Plateau and Gueron 1982) is optimized for detection of the 2′OH proton resonances centered at 6.8 ppm ($\varepsilon \approx 170$ μs at 800 MHz ^{1}H frequency). The low power $90°_{-x}$ ^{1}H pulses of the WATERGATE scheme have durations of 1.5 ms. Phase cycling: $\phi_1 = x$; $\phi_2 = x$; $\phi_3 = x, y, -x, -y$; receiver $= x, -x$. States-TPPI phase cycling of ϕ_1 and ϕ_2 was used to obtain quadrature detection in the ^{1}H (F_1) and ^{13}C (F_2) indirect dimensions, respectively. Delay durations: τ = 50 ms; δ = 3 ms; τ_m = 40 ms; $\Delta_H = (t_2 + PW_{RB})/2$; $\Delta_C = (t_1 - 2\delta - PW_{RB})/2$, where PW_{RB} is the width of the ^{13}C REBURP pulse. Pulsed field z-axis gradients are sine-bell shaped with durations of G_1 = 2.1 ms and G_2 = 0.35 ms and peak amplitudes of 20 G/cm (G_1) and 30 G/cm (G_2). Bruker pulse sequence codes, acquisition parameters, and NMRPipe processing scripts can be downloaded from < http://spin.niddk.nih.gov/bax >

composite adiabatic WURST decoupling (Kupče and Freeman 1995).

At time point b, the ^{15}N–^{1}H MQ coherence is converted to ^{1}H transverse magnetization, anti-phase with respect to the one-bond ^{15}N, which subsequently refocuses during the following δ delay, prior to being stored along the z-axis for NOE mixing. The NOE mixing period is followed by selective detection of $^1H^N$ magnetization using a combination of EBURP2 and REBURP band-selective shaped pulses (Geen and Freeman 1991), yielding adequate water suppression on cryogenic probeheads as well as suppression of the intense signals from protonated detergent.

The MT-PARE concept easily can be extended to more complicated situations in which, for example, homonuclear ^{13}C–^{13}C decoupling is required. In our previous study of the 2′OH group in an A-form RNA, we implemented the PARE strategy in a constant-time manner in order to achieve homonuclear ^{13}C–^{13}C decoupling (Ying and Bax 2006). That study showed NOEs between the H3′ and 2′OH protons in an A-form RNA to be very weak, prohibiting accurate E.COSY type $^3J_{C3'-2'OH}$ measurement from the NOE peak positions. Use of the MT-PARE approach (Fig. 2), lacking the 25-ms constant-time segment required in our original experiment (Ying and Bax 2006), overcomes the sensitivity loss associated with this CT evolution. The first 2δ fraction of ^{1}H chemical shift evolution takes place in a CT fashion (Fig. 2A). Use of the 3 ms REBURP pulse (Geen and Freeman 1991) in the middle of the MQ period for selectively refocusing C3′ magnetization provides an additional short constant-time segment that can be utilized to extend the CT evolution of ^{1}H chemical shifts, even when t_2 = 0. Further constant-time ^{1}H chemical shift evolution is available until t_1 reaches $t_2 + 2\delta + PW_{RB}$, where PW_{RB}

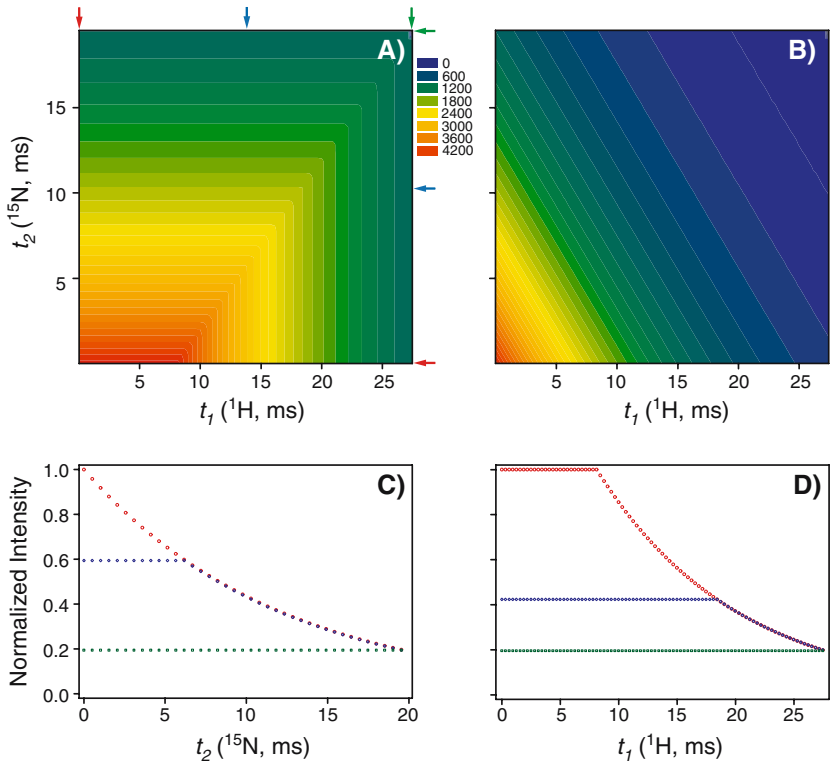

Fig. 3 Intensity plots of the 2D simulated time domain data for (**A**) MT-PARE acquisition, and (**B**) conventional incrementation of t_1 and t_2 durations. Intensity at $t_1 = t_2 = 0$ is identical in both data sets. Representative 1D slices of the simulated PARE data taken at the t_1 (or t_2) points indicated by colored arrows are shown in (**C**) for the ^{15}N dimension and in (**D**) for the ^{1}H dimension in corresponding colors

is the pulse width of the REBURP pulse (Fig. 2B), followed by real-time incrementation when $t_1 > t_2 + 2\delta + \mathrm{PW_{RB}}$ (Fig. 2C). The MT-PARE strategy is also implemented for the ^{13}C chemical shift evolution either in real-time fashion (Fig. 2A, B) or in constant-time manner (Fig. 2C), depending on t_2 relative to t_1. In the case of Fig. 2C when Δ_C is sufficiently long to permit decrementation, ^{13}C chemical shifts are first recorded in a constant-time manner by moving the nonselective 180° ^{13}C pulse toward the selective 180° pulse. Note that the C_3'-selective REBURP pulse is always applied at the center of the PARE period and therefore refocuses all $^{13}C_3'$–^{13}C couplings between time points *a* and *b*, whereas J_{CC} evolution is not affected by the non-selective ^{13}C 180° pulse.

After the MT-PARE evolution, C3′–H3′ MQ coherence is converted to antiphase H3′–{^{13}C3′} magnetization which rephases during the subsequent δ delay, prior to storage along *z* by the 90° ^{1}H pulse that precedes NOE mixing. For our application, interest is on magnetization transfer to the 2′OH protons, which resonate less than 2 ppm downfield of the H_2O resonance. The regular WATERGATE sequence (Piotto et al. 1992), preceded by a jump-and-return 90_{-x}-ε-90_x element (Plateau and Gueron 1982) to ensure H_2O magnetization remains along *z*, is used to read out the final signals.

In order to take optimal advantage of MT-PARE, the experiment should be set up such that the acquisition times in both indirect dimensions during the PARE period are approximately equal. For example, in the application of the MT-PARE strategy to KcsA, the ^{15}N acquisition time was set to ca 19.5 ms (39 points, 514 μs dwell time), this corresponds to 63 points (312 μs dwell time) to be acquired during the PARE evolution for the ^{1}H dimension. Adding the delay period 2δ (ca 8 ms, equivalent to an additional 26 points) finally results in a total acquisition time of 27.5 ms (89 points) in the ^{1}H dimension. The PARE approach therefore not only enhances sensitivity by minimizing relaxation losses, but also yields higher spectral resolution in the indirect ^{1}H dimension than can be obtained by the conventional HMQC-NOESY method, in particular when applied to larger proteins.

Effect of MT-PARE on line shape and intensity

The extent of signal enhancement and line shape distortion resulting from the MT-PARE approach is most easily evaluated by comparing a simulated MT-PARE resonance, chosen to be on-resonance in both dimensions, with the analogous signal acquired in the conventional manner. The time domain data in the two indirect dimensions acquired with the MT-PARE and conventional method are compared in Fig. 3. While the initial intensity, at $t_1 = t_2 = 0$, is identical for both data sets, it is evident that the signal decays much more slowly in the MT-PARE spectrum than in the

conventional one, which underlies the significant sensitivity and resolution enhancement of the MT-PARE approach. Slices for representative FIDs in the ^{15}N and ^{1}H dimensions are shown in Fig. 3C, D. As can be seen in Fig. 3C, the ^{15}N t_2 cross section, taken at a t_1 duration smaller than 2δ (Fig. 1A) exhibit their regular exponential decay because such ^{15}N FIDs require incrementation of the total duration where multiple quantum coherence is present. However, for $t_1 > 2\delta$, the ^{15}N signal initially shows no decay until $t_2 > t_1 - 2\delta$, after which it decays exponentially. For the longest t_1 (^{1}H) evolution duration, the ^{15}N chemical shifts are recorded fully in the constant-time mode, with no signal decay (Fig. 3C).

Similarly, cross sections through the time domain signal taken in the ^{1}H dimension (Fig. 3D), initially (at $t_2 = 0$) are of a constant time nature for a duration 2δ, which increases to $2\delta + t_2$ for later t_2 values, before the signal starts to decay in the t_1 (^{1}H) dimension.

The line shapes corresponding to the time domain data of Fig. 3A, B are obtained by Fourier transformation, after cosine bell apodization and zero filling, and are shown in Fig. 4, together with the 1D slices in both ^{1}H and ^{15}N dimensions. The cross sections show that the peak height in the MT-PARE spectrum is approximately two-fold higher than for the conventional spectrum and that the resolution in the ^{1}H dimension is much improved. Although the precise degree of enhancement attainable with MT-PARE depends on the choice of the acquisition parameters, in all cases MT-PARE outperforms conventional acquisition due to the higher integrated intensity of its time domain signal.

Owing to the non-exponential decay profile of MT-PARE data, its Fourier transformed signal does not exhibit the normal two-dimensional Lorentzian shape. In principle, provided that the ^{1}H single quantum and heteronuclear MQ relaxation times are similar for all signals and approximately known, a special windowing function can be applied to the constant time fraction of the MT-PARE time domain data such that the signal approaches a smooth exponential decay in both dimensions. In practice, however, we find that the simple use of a cosine bell window in both MT-PARE dimensions yields close to optimal results.

Application of 3D MT-PARE HMQC-NOESY to KcsA

We demonstrate the simultaneous enhancements in both sensitivity and resolution attainable with the MT-PARE approach for measurement of H^N–H^N NOEs in the tetrameric KcsA-SDS mixed micelles, which have a total mass of ca 125 kDa. Such NOE information, previously recorded with the conventional type experiments, proved highly useful in confirming backbone assignments as well as characterization of the 3D structure of this protein (Chill et al. 2006b).

Figure 5 compares representative ^{1}H–^{1}H cross-sections taken through the 3D HMQC-NOESY spectra acquired for KcsA with the PARE strategy and the conventional approach. The spectra were recorded in D_2O solution and only contain resonances for amides that are highly protected from hydrogen exchange, and all are located in the transmembrane domain previously solved by X-ray crystallography (Doyle et al. 1998). These amides all exhibit high S^2 order parameters and correspondingly high transverse ^{15}N relaxation rates of ca 55 s^{-1} (Chill et al. 2006a), and therefore pose a challenging problem both in terms of spectral resolution and sensitivity.

Comparison of the conventional and MT-PARE HMQC-NOESY spectra clearly demonstrates the gain in sensitivity as well as improved spectral resolution in the indirectly detected ^{1}H dimension of the spectrum. With the noise levels being identical in the two spectra, the experimentally observed ratio in intensities of 1.7±0.3 directly reflects the increase in signal to noise ratio, which falls slightly below that expected on the basis of the simulations of Fig. 4. The non-uniformity and, on average, slightly smaller than expected gain in signal-to-noise ratio are attributed to variations in the transverse relaxation rates of the various amides. For example, spectra simulated for lower transverse relaxation rates (^{1}H T_2 = 20 ms; ^{1}H–^{15}N MQ T_2 = 24 ms) indicate only 48% sensitivity enhancement, whereas 100% enhancement is obtained for the fast relaxation case (^{1}H T_2 = 10 ms; ^{1}H–^{15}N MQ T_2 = 12 ms). Analogously, we observe smaller gains in sensitivity of ca 1.5±0.2 for KcsA spectra recorded in H_2O, which are dominated by the more slowly relaxing, partially disordered regions of the protein (data not shown).

Application of 3D MT-PARE to the study of H3′–2′OH NOEs in RNA

The MT-PARE experiment of Fig. 2 is demonstrated for observation of H3′–2′OH NOEs in the stem-loop RNA, helix-35ψ, that were previously found to be very weak when using a constant-time PARE experiment (Ying and Bax 2006), and thus represent another situation in which sensitivity enhancement is greatly needed.

Figure 6 compares 2D representative cross sections through the 3D MT-PARE and corresponding con-

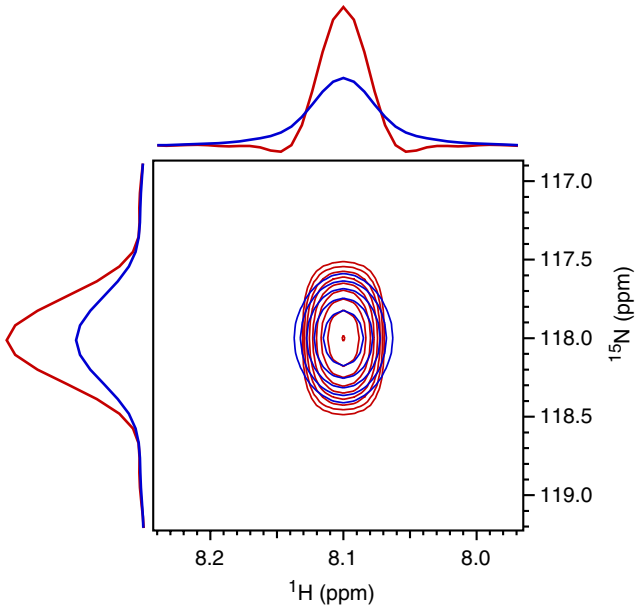

Fig. 4 Overlay of the simulated 2D cross peaks and their on-resonance cross sections for the MT-PARE (red) and conventional (blue) experiments, corresponding to the time domain signals of Fig. 3A, B. Cross sections and lowest contour levels are shown at the same absolute scaling, and therefore reflect the intensity gain in MT-PARE over the conventional approach. Thermal noise, if included in the simulations, would be identical in the two spectra, i.e., the increased intensity directly corresponds to increased signal-to-noise

ventional HMQC-NOESY experiments. Enhancements in signal-to-noise ratio range from 1.2 to 2.0. With a mean increase in signal-to-noise ratio of 1.5 ± 0.3, gains are somewhat lower than for the transmembrane domain of KcsA, primarily resulting from the more favorably relaxation properties of helix-35ψ relative to KcsA, that therefore offer less room for sensitivity enhancement by reducing the apparent relaxation rate. The MT-PARE experiment demonstrated in this study yields NOE cross peaks to 2′OH peaks that are in-phase with respect to C3′. However, as previously demonstrated, the method can be readily extended to obtain 2′OH peaks that are anti-phase with respect to C3′. Sums and differences from such spectra (Ottiger et al. 1998) can then be used to extract $^{3}J_{C3'-2'OH}$ couplings in an E.COSY type manner (Griesinger et al. 1986; Ying and Bax 2006).

Concluding remarks

The concept of MT-PARE is applicable to all 3D and 4D experiments that utilize multiple quantum evolution of isolated two-spin pairs. The approach takes advantage simultaneously of the favorable relaxation properties of heteronuclear multiple quantum coherence and of minimizing the total duration during which spin relaxation is effective. It is worth noting, however, that for cases such as methylene or methyl groups, the multiple quantum approach is often less effective than sequential single quantum evolution because two-spin multiple quantum coherence in a methylene is split by the large $^{1}J_{CH}$ interaction to the second proton. Similarly, for methyl groups the two remaining passive protons result in a triplet splitting when applying the MT-PARE approach, unless partial deuteration is used, together with selection of isolated ^{13}C–^{1}H pairs.

The MT-PARE approach therefore appears best suitable for ‘‘uni-directional’’ experiments where magnetization is transferred from an amide or methine proton to another site in the molecule, either via NOE or a through-bond *J* coupling pathway. Especially when applied to larger systems, such as measurement of H^N–H^N NOEs in tetrameric KcsA, substantial enhancements in sensitivity of up to 100% with concomitantly increased spectral resolution are attainable.

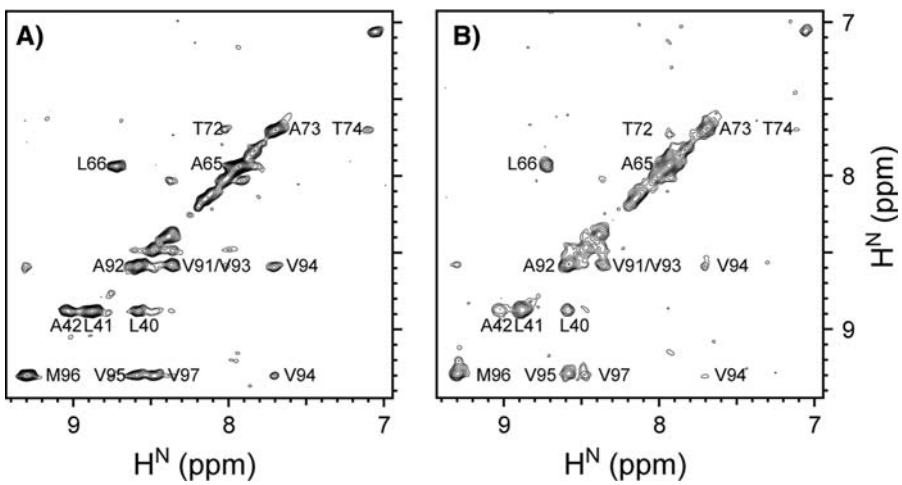

Fig. 5 Two-dimensional (F_1, F_3) cross sections, taken at $F_2(^{15}N)$ = 119.9 ppm, from (**A**) the 3D MT-PARE-HMQC-NOESY and (**B**) the conventional HMQC-NOESY spectrum recorded for KcsA at 50°C, with a NOE mixing time of 80 ms. Spectra are recorded and processed in the same manner, with the lowest contour level set at the same level, and using an identical multiplicative factor of 1.3 between contours

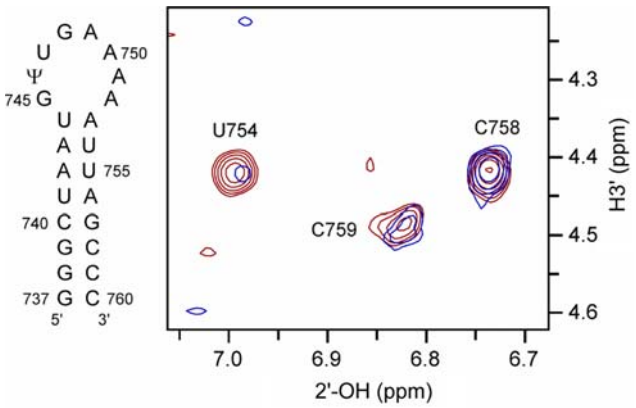

Fig. 6 Representative overlayed two-dimensional (F_1, F_3) cross-sections taken at $F_2(^{13}C3') = 72.1$ ppm from the 3D MT-PARE-HMQC-NOESY (red) and the 3D conventional HMQC-NOESY (blue) spectra recorded for the 24-nt stem-loop RNA, Helix-35ψ, at 7°C with a mixing time of 40 ms. Contours are spaced at a factor 1.3. Note that the correlation of U754 is stronger in adjacent planes, and the 3D peak maximum is 2.0 times higher in the MT-PARE-HMQC-NOESY than in the regular HMQC-NOESY spectrum

Both experimental and simulated results indicate that the gains offered by MT-PARE are largest for systems with short transverse relaxation times, i.e., where the improvement is most needed. Line shape calculations show that the unusual decay envelope of the time domain signal in MT-PARE results in a line shape that has an appearance similar to that when a shifted sine bell is used for enhancing spectral resolution, however without the loss in signal-to-noise ratio associated with such apodization.

Commonly, evolution in the indirectly detected dimension of semi-constant time heteronclear triple resonance experiments has been carried out in such a way that the fraction of incremented time scales linearly with the fraction of the constant time that is used for spin evolution (Grzesiek et al. 1993; Logan et al. 1993), such that signal decay remains exponential. As demonstrated in our present work, it is advantageous in terms of both resolution and sensitivity if first the maximum evolution in the constant-time delay is exploited, prior to incrementation of the delay during which additional relaxation occurs. The gain in both sensitivity and resolution attainable from such a switch in the interval that is being modified during the experiment easily offsets the minor increase in complexity required for coding the required pulse sequence.

Supplementary material

Alternative version of the 3D MT-PARE-HMQC-NOESY pulse schemes presented in Fig. 1; Intensity plot and cross sections of the 2D time domain data simulated using the alternative pulse scheme.

Acknowledgements We thank Ed Nikonowicz (Rice U.) for the Helix-35 RNA sample. This work was supported by the Intramural Research Program of the NIDDK, NIH, and by the Intramural Antiviral Target Program of the Office of the Director, NIH.

References

Bax A, Kay LE, Sparks SW, Torchia DA (1989) Line narrowing of amide proton resonances in 2D NMR-spectra of proteins. J Am Chem Soc 111:408–409

Chill JH, Louis JM, Baber JL, Bax A (2006a) Measurement of 15N relaxation in the detergent-solubilized tetrameric KcsA potassium channel. J Biomol NMR 36:123–136

Chill JH, Louis JM, Miller C, Bax A (2006b) NMR study of tetrameric KcsA potassium channel in detergent micelles. Protein Sci 15:684–698

Delaglio F, Grzesiek S, Vuister GW, Zhu G, Pfeifer J, Bax A (1995) NMRpipe – a multidimensional spectral processing system based on Unix pipes. J Biomol NMR 6:277–293

Doyle DA, Cabral JM, Pfuetzner RA, Kuo AL, Gulbis JM, Cohen SL, Chait BT, MacKinnon R (1998) The structure of the potassium channel: molecular basis of K+ conduction and selectivity. Science 280:69–77

Geen H, Freeman R (1991) Band-selective radiofrequency pulses. J Magn Reson 93:93–141

Griesinger C, Sørensen OW, Ernst RR (1986) Correlation of connected transitions by two-dimensional NMR spectroscopy. J Chem Phys 85:6837–6852

Griffey RH, Redfield AG (1987) Proton-detected heteronuclear edited and correlated nuclear-magnetic-resonance and nuclear Overhauser effect in solution. Q Rev Biophys 19:51–82

Grzesiek S, Anglister J, Bax A (1993) Correlation of backbone amide and aliphatic side-chain resonances in $^{13}C/^{15}N$-enriched proteins by isotropic mixing of ^{13}C magnetization. J Magn Reson Ser B 101:114–119

Grzesiek S, Bax A (1995) Spin-locked multiple quantum coherence for signal enhancement in heteronuclear multidimensional NMR experiments. J Biomol NMR 6: 335–339

Gschwind RM, Gemmecker G, Kessler H (1998) A spin system labeled and highly resolved ed-H(CCO)NH-TOCSY experiment for the facilitated assignment of proton side chains in partially deuterated samples. J Biomol NMR 11:191–198

Ikura M, Kay LE, Bax A (1990) A novel approach for sequential assignment of ^{1}H, ^{13}C, and ^{15}N spectra of larger proteins: heteronuclear triple-resonance three-dimensional NMR spectroscopy. Application to calmodulin. Biochemistry 29:4659–4667

Kupče E, Freeman R (1995) Adiabatic pulses for wideband inversion and broadband decoupling. J Magn Reson A 115:273–276

Logan TM, Olejniczak ET, Xu RX, Fesik SW (1993) A general-method for assigning NMR spectra of denatured proteins using 3D HC(CO)Nh ToCSY triple resonance experiments. J Biomol NMR 3(2):225–231

Marino JP, Diener JL, Moore PB, Griesinger C (1997) Multiple-quantum coherence dramatically enhances the sensitivity of CH and CH_2 correlations in uniformly ^{13}C-labeled RNA. J Am Chem Soc 119:7361–7366

Nikonowicz EP, Sirr A, Legault P, Jucker FM, Baer LM, Pardi A (1992) Preparation of ^{13}C and ^{15}N labelled RNAs for heteronuclear multi-dimensional NMR studies. Nucleic Acids Res 20(17):4507–4513

Ottiger M, Delaglio F, Bax A (1998) Measurement of *J* and Dipolar couplings from simplified two-dimensional NMR spectra. J Magn Reson 131:373–378

Pervushin K, Eletsky A (2003) A new strategy for backbone resonance assignment in large proteins using a MQ-HACACO experiment. J Biomol NMR 25:147–152

Piotto M, Saudek V, Sklenár V (1992) Gradient-tailored excitation for single-quantum NMR spectroscopy of aqueous solutions. J Biomol NMR 2(6):661–665

Plateau P, Gueron M (1982) Exchangeable proton NMR without base-line distortion, using new strong-pulse sequences. J Am Chem Soc 104:7310–7311

Shang Z, Swapna GVT, Rios CB, Montelione GT (1997) Sensitivity enhancement of triple-resonance protein NMR spectra by proton evolution of multiple-quantum coherences using a simultaneous ^{1}H and ^{13}C constant-time evolution period. J Am Chem Soc 119:9274–9278

Ying J, Bax A (2006) Determination of 2′-OH proton positions in helical RNA by simultaneously measured heteronuclear scalar couplings and NOEs. J Am Chem Soc 128:8372–8373